Available online at www.sciencedirect.com
SCIENCE DIRECT®
Catalysis Today 97 (2004) 145–151
CATALYSIS TODAY
www.elsevier.com/locate/cattod

Recent advances in nano precious metal catalyst research at Union Chemical Laboratories, ITRI

Wu-Hsun Cheng*, Kao-Ching Wu, Man-Yin Lo, Chiou-Hwang Lee

Union Chemical Laboratories (UCL), Industrial Technology Research Institute (ITRI), 321 Kuang Fu Road, Sec. 2, Hsinchu, Taiwan 300, ROC

Received 18 November 2003; received in revised form 25 February 2004; accepted 22 March 2004
Available online 27 September 2004

Abstract

This study illustrates some recent progress of nano precious metal catalyst research at Union Chemical Laboratories (UCL). Nano gold catalyst was prepared by a precipitation method, in which, $HAuCl_4$ was precipitated onto a suspension of the iron hydroxide support, with a low calcination temperature at 453 K. The catalysts were highly active with 100% conversion achieved for the oxidation of carbon monoxide (CO) within 10,000 ppm at ambient temperature and high space velocity up to 500,000 h^{-1}. This catalyst had good lifetime and was resistant to moisture and high concentration of CO_2. In addition, Pt–Ru/C catalyst for direct methanol fuel cell was prepared with the high surface area mesoporous carbon support and possesses both uniform dispersion of precious metals and very small crystallite size. Catalyst prepared using the incipient-wetness method resulted in the formation of extremely active Pt–Ru/C catalysts. The enhancement in activity is mainly attributed to the intimate contact of Pt and Ru that forms the dual active site.

Keywords: Nanocatalyst; Gold catalyst; CO oxidation; Direct methanol fuel cell (DMFC); Pt–Ru/C

1. Introduction

Nanotechnology has great impact on materials, microelectronics, computing, pharmaceutical, biochemistry, environmental, energy and chemical industries. Not only is nanocatalyst an important part of nanotechnology, but also catalysis and nanotechnology could complement each other. For example, catalysts can be used to facilitate the production of some nanotech products such as carbon nanomaterials and polymer/clay nanocomposites [1]. On the other hand, nanomaterials may also be used to combine with catalysts or adsorbents to achieve some interesting features [1]. Some recent advances in nanocatalysts at Union Chemical Laboratories (UCL) has been described in this paper.

Gold (Au) has long been considered as an inert metal until, Haruta et al. [2] discovered in 1987 that it exhibits extraordinary catalytic activities under certain conditions. When nano-sized gold particle is dispersed on oxide carriers [3–11], it becomes an excellent catalyst for the oxidation of carbon monoxide (CO), even under ambient conditions. Although, the use of deposition–precipitation (DP) and chemical vapor deposition (CVD) methods are capable of forming gold particles of grain size between 2 and 10 nm, agglomeration of Au particulates takes place easily, which resulted in the rapid deactivation of catalyst [2,12–14]. In this study, an active catalyst for CO oxidation was prepared by a precipitation method, in which the $HAuCl_4$ was precipitated onto a suspension of the iron hydroxide and nano-TiO_2 support. In order to suppress the deactivation of supported gold catalyst due to active site agglomeration, UCL has devoted extensive efforts to improve the interaction between gold and the support, in order to, alleviate the chance of active site agglomeration. The catalyst has passed the tests regarding the catalyst lifetime and resistance to high concentrations of moisture and CO_2.

Another nanocatalyst that is going to have a major impact is the Pt–Ru based catalyst used in direct methanol fuel cell (DMFC). Owing to the simplicity in structure and inherent

* Corresponding author. Tel.: +886 3 5732001; fax: +886 3 5732000.
E-mail address: cheng@itri.org.tw (W.-H. Cheng).

0920-5861/$ – see front matter © 2004 Elsevier B.V. All rights reserved.
doi:10.1016/j.cattod.2004.03.065

high power density, DMFC is considered as the most possible candidate, as a low-to-medium power electric power device for portable application [15], and device that requires high power density. At present, the two most serious technical hurdles for the commercialization of DMFC are inadequate activity of the anode catalysts and methanol leakage through the electrolyte membrane. DMFC employs methanol as the direct fuel; methanol oxidation at the anode is the rate-limiting factor for the performance of the fuel cell. The main reason for such limitation is mainly due to the poor kinetics of methanol oxidation at the anode. This poor kinetics is because of the slow oxidation rate of CO intermediate formed from the activation of methanol on Pt active sites [16]. The development of a more active and durable anode catalyst has become one of the most essential issues towards the realization of DMFC. Pt–Ru/C bimetallic catalyst is currently the state of the art anode catalyst for DMFC. Pt and Ru metals located next to each other forms the dual active site, which is needed for methanol conversion [17]. The methods employed for the preparation of electrocatalysts strongly affect the dispersion and compositional homogeneity of active sites, both of which determine the catalytic activity of methanol oxidation. In the present study, a preparation method that favors the formation of more homogeneous distribution of Pt and Ru was explored for the preparation of Pt–Ru/C catalysts. Transmission electron microscopy (TEM), CO chemisorption, EXAFS, and BET were used as the characterization tools and cyclic voltammetry (CV) was used to probe the activity of catalyst towards methanol oxidation.

2. Experimental

2.1. Gold catalyst

The iron hydroxide support was prepared by a precipitation method using $FeCl_3{\cdot}6H_2O$ and 30% ammonia solution. The final pH value of the solution was controlled to be 10. The obtained mixture was filtered and washed with de-ionized water to remove the chlorine ions, followed by drying at 110 °C to obtain $Fe(OH)_x$.

The titanium hydroxide support was prepared by a precipitation method using $TiCl_4$ and 30% ammonia solution. The final pH value of the solution was controlled to be 10. The obtained mixture was filtered and washed with de-ionized water to remove the chlorine ions, followed by drying at 110 °C to obtain $Ti(OH)_x$. The nano-TiO_2 support was prepared by a hydrothermal treatment at 100 °C. Seventy per cent of nitric acid aqueous solution was used to adjust the pH value of the mixture to 2. The obtained mixture was filtered and dried at 110 °C to obtain nano-TiO_2.

Gold supported on either iron hydroxide or nano-TiO_2 was prepared by precipitation of an aqueous solution of $HAuCl_4$ onto either $Fe(OH)_x$ or nano-TiO_2. An ammonia solution was used to adjust the pH value. The final pH value of the solution was controlled to be 10. After precipitation, the catalyst precursor was filtered and washed with de-ionized water to remove the chloride ions, followed by drying at 110 °C and calcination at 150–350 °C.

The catalysts were characterized by N_2 sorption (Micromeritics ASAP2000), TEM (Jeol FS2000), ICP-AES (Perkin Elmer OPT 1MA 3000DV) and X-ray diffraction (Shimadzu XD-D1). XRD measurements were performed using a Shimadzu XD-D1. XRD line broadening was used to calculate the average crystallite size using the Scherrer equation. TEM experiments were performed using a Jeol FS2000 microscope. The energy of the incident electrons was 300 kV. The Au loading was determined by ICP-AES.

Carbon monoxide (CO) oxidation was used to probe the performance of the gold catalysts prepared in this study. Catalyst activity was measured in a quartz fixed-bed reactor with 6 mm diameter. Five hundred milligrams of 30–40 mesh catalyst was used for all activity measurements at ambient temperature of about 25 °C, unless, otherwise indicated. The catalyst was pre-treated in an air stream at 180 °C for 4 h before the reaction gas with various CO concentrations was passed through the catalytic bed. The catalyst temperature was monitored with a quartz-tube covered thermocouple in contact with the inlet of the catalyst bed. The composition of the reaction mixture was controlled using mass flow controllers. High concentration of CO in the outlet gas was analyzed by a Rosemount analytical CO analyzer (Model 880A with the detection range of 0.01–20%). A CO detector from Industrial Scientific Co. (the detection range of 0–1999 ppm) was used for low concentration analysis. Calibration was performed using a standard gas containing known concentrations of the components.

2.2. Pt–Ru/C catalyst

Mesoporous (CMK-1) carbon was prepared using MCM-41, as the template according to Joo et al. [18]. Carbon supported Pt–Ru binary metal catalysts (Pt–Ru/C) were prepared using DP [19] and incipient wetness (IW) methods. Precursors used for catalyst preparation were $Pt(NO_2)_2(NH_3)_2$ and $Ru(NO)(NO_3)_3$. Both commercial carbon black (Cabot Vulcan XC-72) and in-house mesoporous carbon were used as the catalyst carriers. In the IW method, carbon support in a round-bottom flask was evacuated before an aqueous solution containing both $Pt(NO_2)_2(NH_3)_2$ and $Ru(NO)(NO_3)_3$ were added, until wetting of the support is observed. The amount of precursor solution used for catalyst preparation is equivalent to the pore volume of the support employed for the preparation of catalyst. Removal of solvent from the wetted support was facilitated by vacuum drying. Further drying at 120 °C resulted in the formation of the catalyst precursor. The catalyst precursor was then reduced in 10% hydrogen in nitrogen at 200 °C for 2 h, before use. Metal loading of the

catalysts was varied, while the atomic ratio of Pt/Ru was kept at 1:1, unless, otherwise indicated. Commercial catalysts were obtained from Johnson–Matthey and E-Tek.

Transmission electron microscopy (TEM), XRD, and BET were used for the characterization of Pt–Ru/C catalyst using the same instruments described in Section 2.1. A beaker-type electrochemical cell equipped with the working electrode, a platinum mesh counter electrode and an Ag/AgCl reference electrode was used for all electrochemical measurements according to Takasu et al. [20]. The cell was purged with nitrogen to remove dissolved oxygen from the methanol solution. All potentials throughout this paper are referred to the reference hydrogen electrode (RHE) scale. CO stripping voltammetry [15] and catalyst activity measurements were recorded at ambient temperature and 60 °C using an Autolab PGSTAT 30 Potentiostat. The electrochemical oxidation of methanol was characterized by the steady-state current density at 0.5 V in 1.0 M CH_3OH/0.5 M H_2SO_4 solution.

3. Results and discussion

3.1. Gold catalyst

XRD patterns revealed that the nano-TiO_2 support prepared in this study has an anatase crystallite phase. These results also showed that the metal crystallite size was around 8 nm, as calculated from the Scherrer equation. In addition, BET data revealed, that this support has a surface area of 160 $m^2\ g^{-1}$. On the other hand, the iron hydroxide support was found to have a particle size of smaller than 20 nm and surface area of 250 $m^2\ g^{-1}$, as revealed by TEM and BET, respectively. It should be noted that the iron hydroxide support was prepared at pH value of 10 and calcined at 180 °C. Under these conditions, nano-sized iron hydroxide was obtained, which is believed to be important for the formation of homogeneous dispersion of nano-sized gold. The use of either lower pH value or higher calcination temperature results in the formation of iron hydroxide with much larger particle size. Our results showed that iron hydroxide of large particle size is not a good support for gold metal. Okumura et al. [21] have reported that the optimum calcination temperature depends on both the nature of the metal oxide supports and preparation methods used.

Fig. 1 shows the XRD diffraction patterns of the gold catalysts calcined at different temperatures. These results revealed that both iron hydroxide and α-Fe_2O_3 co-existed, when the calcination temperature was higher than 250 °C. When the calcination temperature was lower than 200 °C, formation of amorphous catalyst support was observed. Calcination of the catalysts at high temperature should be avoided, as it could lead to the formation of iron oxide and loss of surface area. Characteristic XRD peaks for gold were not observed in the spectra, which suggested the crystallite sizes of gold were too small to be detectable by XRD. TEM photograph in Fig. 2 shows that very small gold particles are dispersed on the iron hydroxide support. The particle size of gold metal was about 3 nm

Activity data in Table 1 revealed that both the morphology and the particle size of the TiO_2 support affects the performance of Au catalyst. When mesoporous and anatase TiO_2 support with surface area higher than 200 $m^2\ g^{-1}$ was used, 1 g of this catalyst (3%Au/nano-TiO_2) is capable of completely oxidizing 5 l min^{-1} of 2,500–10,000 ppm CO in air under ambient condition. In addition, the 3% Au/$Fe(OH)_x$ catalyst is capable of completely oxidizing CO in the concentration range of 1,000–10,000 ppm at gas hourly space velocity (GHSV) lower than 500,000 h^{-1}, as shown in Fig. 3. These results clearly demonstrated that both 3% Au/$Fe(OH)_x$ and 3% Au/nano-TiO_2 catalysts are very effective for the oxidation of CO at ambient temperature. The stability study also revealed that CO conversion was maintained at 100% for 100 h on-stream as shown in Fig. 4.

Moisture is an unavoidable component in practical environment that could affect the performance of the catalyst during the oxidation of CO. It was reported that moisture enhanced the activity of Au/Fe_2O_3 catalyst [22,23]. On the contrary, moisture has no or negative effect on Au/$Fe(OH)_3$ catalyst [11,24]. The concentration of moisture was in the range of a few percent under ambient conditions. This concentration is enough to cause the adsorption of water on the catalyst surface under ambient conditions. Furthermore, it has been reported [21] that the moisture in air would also

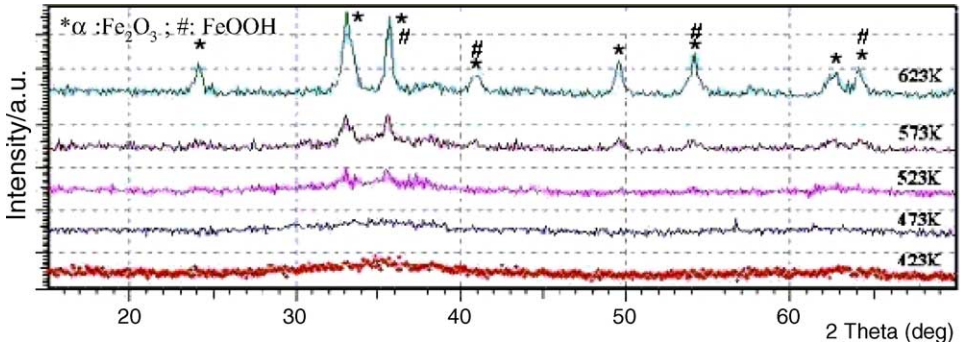

Fig. 1. XRD patterns of 3% Au/$Fe(OH)_x$ catalysts (calcined at 423–623 K, 4 h).

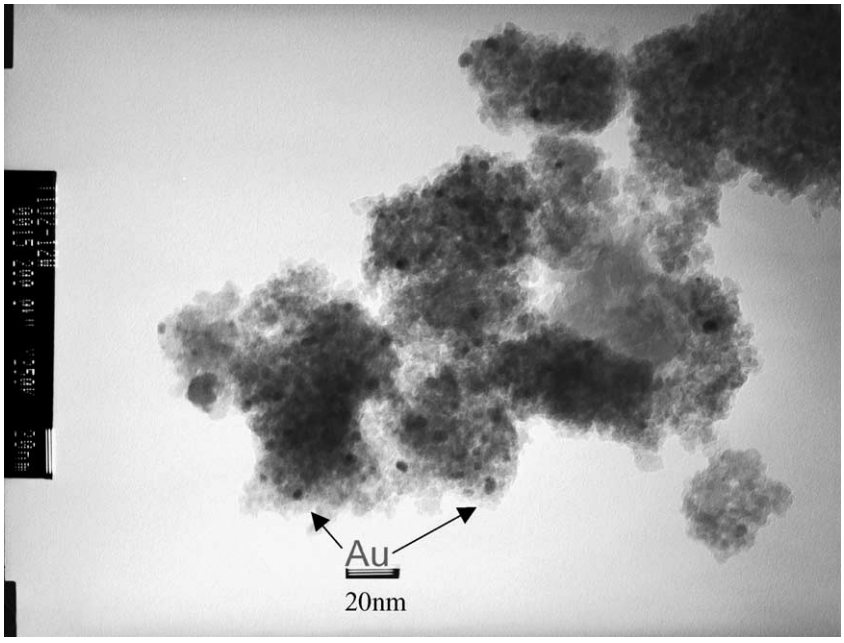

Fig. 2. TEM picture of 3% Au/Fe(OH)$_x$ catalyst (calcined at 180 °C, 4 h).

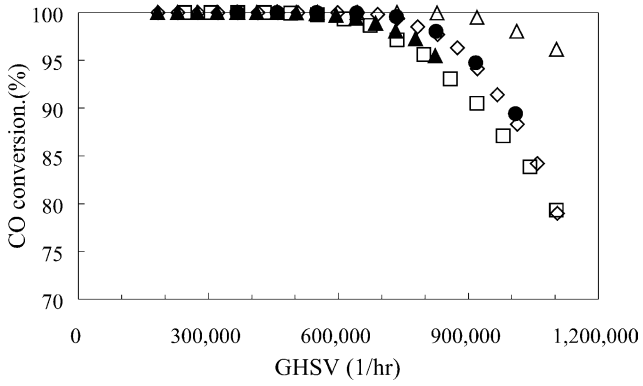

Fig. 3. Activity of 3% Au/Fe(OH)$_x$ catalyst for CO oxidation at ambient temperature. Inlet CO concentration (ppm):(◇) 1000, (△) 2500, (●) 5000, (□) 7500, (▲) 10,000.

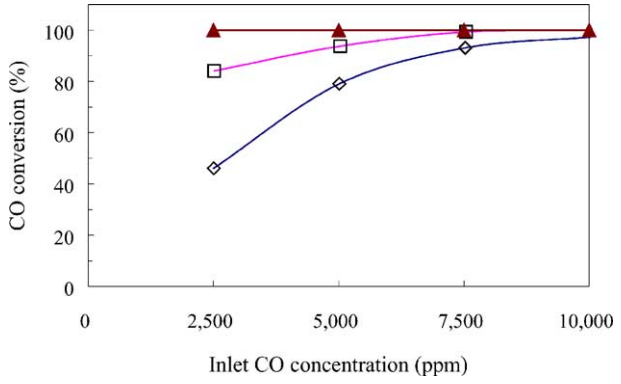

Fig. 5. Effect of CO concentrations and space velocity for 3% Au/Fe(OH)$_x$ catalyst at 25 °C. Reactant gas with saturated moisture. Space velocity (h^{-1}): (▲) 120,000, (□) 200,000, (◇) 400,000.

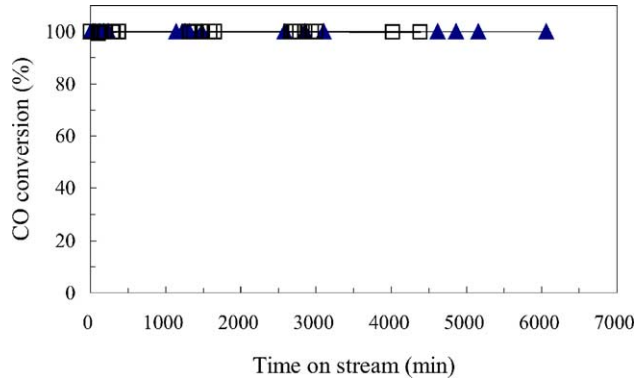

Fig. 4. Durability test of the 3% Au/Fe(OH)$_x$ catalyst. (◆) GHSV 37,600 h^{-1}, CO 2000 ppm, 18 °C. (■) GHSV 38,900 h^{-1}, CO 4000 ppm, 28 °C, saturated moisture.

adsorb on the surface of gold catalysts that caused the loss of catalyst activity. Increasing the CO concentration improved the moisture resistance of the catalyst. The result of the resistance to moisture of the catalyst is shown in Fig. 5. Separate studies show that 100% CO conversion was achieved at these conditions without moisture. The effect of moisture on catalyst performance depends on the CO concentration of the reactant stream. At high GHSV (200,000–400,000 h^{-1}), the effect of saturated moisture becomes more pronounced at lower CO concentration. More heat would be released at higher CO concentration. Heat release would increase the surface temperature of the catalyst and reduce the moisture effect. CO concentration at 4000 ppm was used for catalyst durability test. After continuous operation in the air with saturated moisture, the

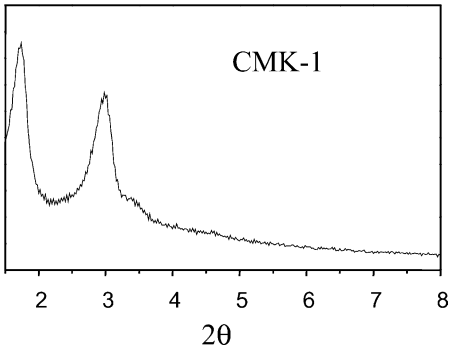

Fig. 6. XRD patterns of CMK-1 support.

conversion of CO over the nano-gold catalyst was still 100% after 4000 min, as shown in Fig. 4. Separate studies also showed, that the catalyst is resistant to 20% CO_2, that is required by the European EN403 Standard.

3.2. Pt–Ru/C catalyst

By using MCM-41 as the template, mesoporous carbon with very high surface area was prepared. Fig. 6 illustrates the XRD pattern of the mesoporous carbon prepared in this study that confirmed the formation of the CMK-1 structure [18]. The BET surface area of 1643 $m^2 g^{-1}$ of this CMK-1 mesoporous carbon is more than six times higher than the commercial Vulcan XC-72 carbon black (S.A. = 254 $m^2 g^{-1}$). Figs. 7 and 8 show the TEM images of Pt–Ru/C catalysts obtained by the IW method using CMK-1 and XC-72 as the supports, respectively. Smaller size of metal particles was obtained with mesoporous carbon support (2.1 nm of Pt–Ru in Fig. 7), than with XC-72 supported catalyst (2.7 nm of Pt–Ru in Fig. 8). In addition, the TEM images also revealed that the metal particles were uniformly dispersed on the CMK-1 support. These results clearly demonstrated that supported catalyst with better dispersion and smaller particle size can be obtained over support with high surface area of CMK-1.

Fig. 9 shows the Pt-L_{III} edge EXAFS Fourier transforms spectra for the Pt–Ru/C (XC-72) catalysts prepared by the DP and IW methods. Two distinct peaks corresponding to the Pt–Ru and Pt–Pt active sites are observed. Comparing the ratio of Pt–Ru to Pt–Pt, peak areas revealed that the IW catalyst has a higher Pt–Ru to Pt–Pt ratio, than the DP catalyst. These results suggested that the IW method is a better method for the preparation of more homogeneously mixed metal atoms than the commonly employed DP method for the preparation of Pt–Ru/C electrocatalyst.

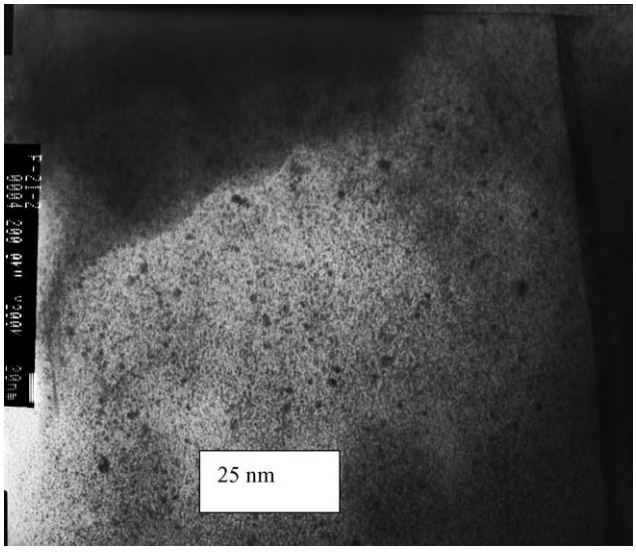

Fig. 7. TEM picture of Pt–Ru/C (CMK-1).

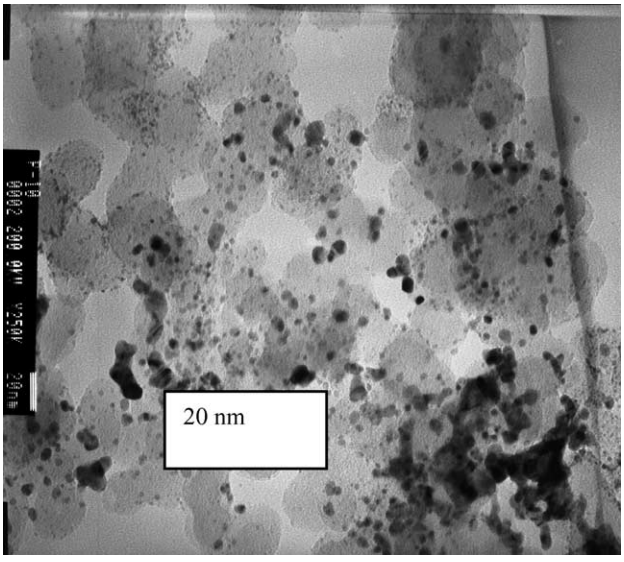

Fig. 8. TEM picture of Pt–Ru/C (Vulcan XC-72).

Table 2 shows the activity and properties of Pt–Ru/C catalysts prepared by the DP and the IW methods with metal loading of 30% (Pt–Ru = 1:1 atomic ratio). Higher current

Table 1
Characteristics of supported gold catalysts

Support	Au loading (wt.%)	Crystallite phase	Surface area ($m^2 g^{-1}$)		Pore size, nm (BJH)	Porosity, (ml g^{-1})	Catalytic activity[a] SV (ml $g^{-1} h^{-1}$)
			BET	Langmuir			
$Fe(OH)_x$	3	Amorphous	250	360	3–4	0.28	500,000
Nano-TiO_2	3	Anatase	160	225	~6	0.23	377,000

Catalyst: 500 mg, CO in air 10,000 ppm (air: dew point in 273 K) at 23–25 °C.
[a] The maximum space velocity achieved at the 100% CO conversion.

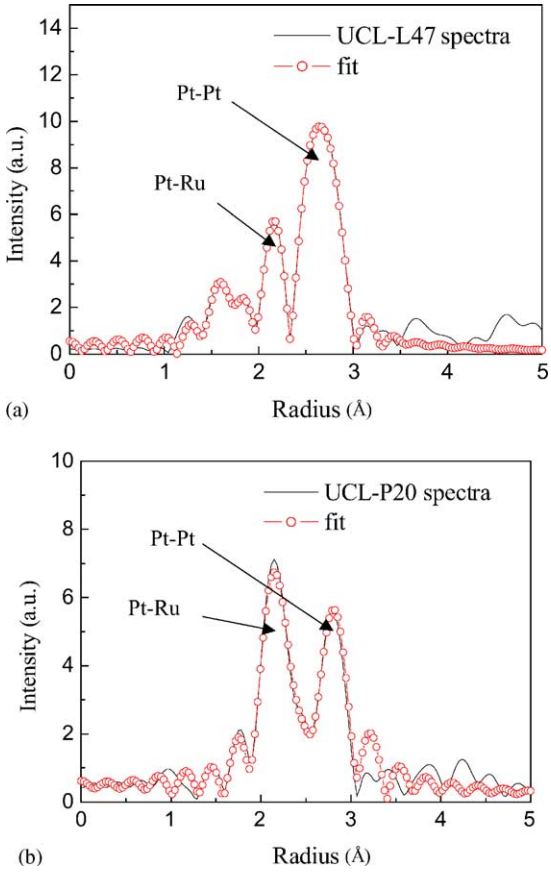

Fig. 9. (a) Fourier transforms of the EXAFS spectra of Pt–Ru/C catalyst prepared by the deposition–precipitation method. (b) Fourier transforms of the EXAFS spectra of Pt–Ru/C catalyst prepared by the incipient wetness (IW) method.

Table 2
Effect of preparation method on activity and metal particle size of the Pt–Ru/C catalysts (ambient temperature)

Catalyst	Support	Method	Loading (wt.%)		Current density	Particle size (nm)
			Pt	Ru	(mA/Pt–Ru (mg))	
UCL-L47	XC-72	DP	21.9	9.1	61.9	2.1
UCL-P20	XC-72	IW	21.0	10.9	83.4	2.7

density was obtained for the IW catalyst. The higher activity of the IW catalyst can be related to its higher amount of Pt–Ru dual sites as revealed by the EXAFS data. These results clearly demonstrated that more homogeneous mixing of Pt and Ru metals is needed for the higher activity of the catalyst. These results also agree well with the dual active site mechanism for the anodic electroxidation of methanol [17]. For the dual site mechanism, Pt active site is responsible for the activation of methanol to form CO intermediate. On the other hand, the Ru active site is responsible for the activation of water to form active hydroxyl group. In order for the efficient conversion of methanol to form CO_2, proton and electron, Pt and Ru active sites must be situated next to each other to form the dual active site. In the presence of the dual active site, CO formed from the activation of methanol over Pt can react with the neighboring Ru activated hydroxyl group to complete the anodic oxidation of methanol. Although, the IW catalyst has a larger metal size than the DP catalyst, it is more active than the DP catalyst because it has more Pt–Ru active sites. The formation of Pt–Ru active sites was affected by the preparation method. The IW method is more suitable than the DP method for the preparation of DMFC catalyst.

Table 3 shows the activity of IW Pt–Ru/C catalysts with different metal loading on the commercial XC-72 support. TEM data revealed that the particle size of metal increases when the loading is increased from 15 to 45%. This increase in particle size suggested that the extent of metal agglomeration increases as the loading of metal is increased. CO stripping data also showed that the metal surface area of the catalyst is decreased as the metal loading is increased. These results clearly demonstrated that the dispersion of metal is decreased as the metal loading is increased. EXAFS data revealed that catalysts with higher metal loading possess higher density of Pt–Ru dual active sites. Results in Table 3 showed that the highest specific activity was observed for the catalyst with 45% loading and the lowest for the one with 15% loading. Although, the catalyst with 15% loading possesses the highest metal surface area and smallest metal particle size, it has the lowest activity among the three catalysts tested. These results suggested that the metal dispersion is not the dominating factor determining the activity of the catalyst for the electro-oxidation of methanol. The results also re-affirmed the dual-site role for methanol oxidation, in which Pt–Ru active site is needed for the effective conversion of methanol.

Table 4 shows the activity data obtained from commercial catalysts, as well as, catalysts prepared by the IW method using conventional carbon black as the support. The

Table 3
Effect of precious metal loading on the physical property and activity of UCL catalysts at 60 °C

Catalyst	Pt–Ru loading (%)	Metal surface area ($m^2\ g^{-1}$)[a]	Particle size (nm)[b]	Pt–Ru/Pt–Pt ratio[c]	Current density (mA mg $metal^{-1}$)
C1	15	92.5	< 2.0	1.58	100
C2	30	71.9	2.4	2.18	153
C3	45	49.2	2.7	2.28	213

[a] By CO-stripping.
[b] By TEM.
[c] By EXAFS.

Table 4
Comparing activities of UCL catalysts with commercial catalysts at 60 °C

Catalyst	Loading (wt.%)			Ru/Pt (atomic ratio)	Current density (mA/mg Pt–Ru)	Particle size (nm)
	Total	Pt	Ru			
E.TEK[a]	39.8	26.3	13.5	1.0	112.5	2.5
JM-H7000[a]	45.0	30.0	15.0	1.0	168.6	2.2
C4	15.0	9.9	5.1	1.0	70.0	2.0
C5	30.0	19.8	10.2	1.0	198.1	2.0
C3	45.0	30.0	15.0	1.0	213.0	2.7

[a] Commercial catalyst.

prepared catalysts were activated in 10% H_2/N_2 at 200 °C for 2 h before the activity test. Higher current densities were obtained from the IW catalyst than commercial catalysts. The IW method in this study produces abundant dual active sites and shows superior catalyst performance.

4. Conclusion

Catalytic oxidation of CO at ambient temperature has been studied over Au/Fe hydroxide catalysts. The catalyst was prepared by a precipitation method, in which $HAuCl_4$ was precipitated onto a suspension of the iron hydroxide support, with a low calcination temperature at 453 K. The catalysts were highly active with 100% conversion achieved for the oxidation of CO within 10,000 ppm at ambient temperature and high space velocity up to 500,000 h^{-1}. This catalyst had good lifetime and was resistant to moisture and high concentration of CO_2.

Mesoporous carbon of high surface area was prepared in this study. Pt–Ru/C catalyst prepared with this high surface area mesoporous carbon possesses both uniform dispersion of precious metals and very small metal size. Catalyst prepared using the IW method resulted in the formation of extremely active Pt–Ru/C catalysts. The improvement in activity is mainly attributed to the intimate contact of Pt and Ru that forms the dual active site.

References

[1] C.H. Lee, W.H. Cheng, S.J. Huang, C. Ting, M.Y. Lo, Proceedings of the Third Conference of the Indo–Pacific Catalysis Association, Taipei, 16–18 November, 2003, KL-A-01.
[2] M. Haruta, T. Kobayashi, H. Sano, N. Yamada, Chem. Lett. 405 (1987).
[3] G.C. Bond, D.T. Thompson, Catal. Rev. Sci. Eng. 41 (1999) 319.
[4] G.C. Bond, D.T. Thompson, Gold Bull. 33 (2000) 41.
[5] G.C. Bond, Catal. Today 72 (2002) 5.
[6] D.T. Thompson, Gold Bull. 31 (1998) 111.
[7] D.T. Thompson, Gold Bull. 32 (1999) 12.
[8] M. Haruta, M. Date, Appl. Catal. A. 222 (2001) 427.
[9] M. Haruta, Catal. Today 36 (1997) 153.
[10] R. Grisel, K.J. Weststrate, A. Gluhoi, B.E. Nieuwenhuys, Gold Bull. 35 (2002) 39.
[11] H. Liu, A.I. Kozlov, A.P. Kozlova, T. Shida, Y. Iwasawa, Phys. Chem. Chem. Phys. 1 (1999) 2851.
[12] M. Haruta, N. Yamada, T. Kobayashi, S. Ijima, J. Catal. 115 (1989) 301.
[13] M. Haruta, S. Tsubota, T. Kobayashi, H. Kageyama, M.J. Genet, B. Delmon, J. Catal. 144 (1993) 175.
[14] A.I. Kozlov, A.P. Kozlova, H. Liu, Y. Iwasawa, Appl. Catal. A. 182 (1999) 9.
[15] A.S. Arico, S. Srinivasan, V. Antonucci, Fuel Cells 1 (2001) 133.
[16] C.L. Green, A. Kucernak, J. Phys. Chem. B 106 (2002) 1036.
[17] T. Schultz, S. Zhou, K. Sundmacher, Chem. Eng. Technol. 12 (2001) 1223.
[18] H.S. Joo, S.J. Choi, I. Oh, J. Kwak, Z. Liu, O. Terasaki, R. Ryoo, Nature 412 (2001) 169.
[19] A.S. Arico, P.L. Antonucci, E. Modica, V. Baglio, H. Kim, V. Antonucci, Electrochim. Acta 47 (2002) 3723.
[20] Y. Takasu, W. Kawaguchi, W. Sugimoto, Y. Murakami, Electrochim Acta 48 (2003) 3861.
[21] M. Okumura, S. Tsubota, M. Haruta, J. Mol. Catal. A Chem. 199 (2003) 73.
[22] M. Haruta, T. Takase, T. Kobayashi, S. Tsubota, in: S. Yoshida, N. Takezawa, T. Ono (Eds.), Catalytic Science and Technology, vol.1, Kodansha, Tokyo, 1991, p. 331.
[23] A.P. Kozlova, A.I. Kozlov, S. Sugiyama, Y. Matsui, K. Asakura, Y. Iwasawa, J. Catal. 181 (1999) 37.
[24] M. Date, Y. Ichihashi, T. Yamashita, A. Chiorino, F. Boccuzzi, M. Haruta, Catal. Today 72 (2002) 89.